Synthesis, Characterisation and DFT Studies of Stigmasterol Mediated Silver Nanoparticles and Their Anticancer Activity

K. Kanagamani, P. Muthukrishnan, M. Ilayaraja, K. Shankar & A. Kathiresan

Journal of Inorganic and Organometallic Polymers and Materials

ISSN 1574-1443
Volume 28
Number 3

J Inorg Organomet Polym (2018)
28:702-710
DOI 10.1007/s10904-017-0721-7

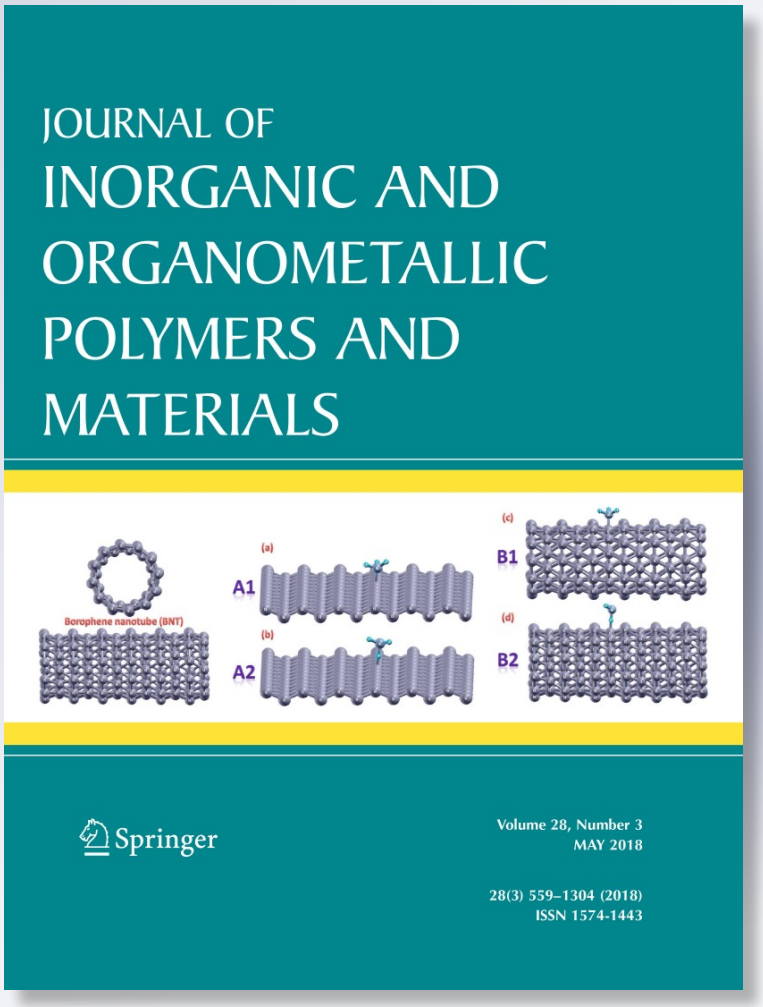

Springer

Your article is protected by copyright and all rights are held exclusively by Springer Science+Business Media, LLC. This e-offprint is for personal use only and shall not be self-archived in electronic repositories. If you wish to self-archive your article, please use the accepted manuscript version for posting on your own website. You may further deposit the accepted manuscript version in any repository, provided it is only made publicly available 12 months after official publication or later and provided acknowledgement is given to the original source of publication and a link is inserted to the published article on Springer's website. The link must be accompanied by the following text: "The final publication is available at link.springer.com".

Author's personal copy

J Inorg Organomet Polym (2018) 28:702–710
DOI 10.1007/s10904-017-0721-7

Synthesis, Characterisation and DFT Studies of Stigmasterol Mediated Silver Nanoparticles and Their Anticancer Activity

K. Kanagamani[1,2] · P. Muthukrishnan[2] · M. Ilayaraja[3] · K. Shankar[2] · A. Kathiresan[2]

Received: 9 September 2017 / Accepted: 21 October 2017 / Published online: 25 October 2017
© Springer Science+Business Media, LLC 2017

Abstract The present investigation reports the facile, reproducible and eco-friendly biological synthesis of nano silver using *Ficus Hispida* leaf extract (FHLE) as a reductant. The properties of the synthesized silver nanoparticles (Ag-NP's) is characterized by scanning electron microscopy, energy dispersive X-ray spectroscopy, transmission electron microscopy (TEM), UV–visible spectroscopy, Fourier transform infrared spectroscopy and X-ray diffraction studies. The synthesized Ag-NPs are found to have spherical shape with average particle size in the range of 50–100 nm. The XRD studies and selected area electron diffraction pattern of TEM images confirm the face cantered cubic structure of biosynthesised silver nanoparticles. The DFT studies reveal that the stigmasterol present in FHLE is responsible for leaf extract to behave as a reducing agent for reduction of Ag^{+} ions into Ag^{0}. The antitumor studies against DLA cell lines of the biosynthesized Ag-NPs is found to have 100% inhibition with concentration of 200 µg/ml of Ag-NP's.

Keywords Silver nanoparticles · *Ficus Hispida* · DFT studies · Cytotoxicity activity

✉ P. Muthukrishnan
mukepmk@gmail.com

[1] Department of Chemistry, SNS College of Technology, Coimbatore 641035, India

[2] Department of Chemistry, Faculty of Engineering, Karpagam Academy of Higher Education, Karpagam University, Coimbatore 641021, India

[3] Department of Chemistry, Arumugam Pillai Seethai Ammal College, Tirupattur 630 211, India

1 Introduction

Metal nanoparticles finds highlighted applications on the various fields of medicinal research because metal nanoparticles show unique and comparably better physical, chemical and biological properties than their macroscopic counterparts due to high surface to volume ratio. The widely used metal nanoparticles in medicinal research are those derived from the valuable metals such as silver [1], gold [2] and platinum [3].The different morphological feature of metal nanoparticles finds applications in the various fields such as environmental chemistry, material science, diagnosis and treatment of diseases [4–6]. Several methods have been employed for synthesising of silver nanoparticle [7]. Maribel et al. reported the synthesis of silver nanoparticles by reduction in solutions [8]. Decomposition of silver compounds by heat [9] is reported by Navaladian et al., Sreeram et al. worked on the microwave assisted synthesis [10], laser mediated synthesis [11], and biological reduction methods [12]. Synthesis of silver nanoparticles from plant species is widely accepted because of its cost effective, environmentally friendly and plants are widely distributed with a range of metabolites. As compared to the available methods, the biosynthesis application would provide better advancement due to its low cost, eco-friendly, low environmental impact and single step synthesis without involving any hazardous solvents. *Ficus Hispida* (FH) belongs to the family of Moraceae and it is commonly known as a devil fig, hairy fig etc. In Tamil the plant is known as peyatti. FH is a moderate size tree known for its edible fruits and folklore value. Traditionally, the different parts of the plant are known to have medicinal activity and widely used for treatment of various diseases like ulcers, psoriasis, anaemia, diabetes, convulsion, hepatitis, dysentery etc. FH is found to possess bioactive groups like alkaloids, sterols, phenols, flavonoids,

Author's personal copy

gums and mucilage, glycosides, saponins and terpenes. Hence FH leaf extract (FHLE) can be used as a reducing agent for biosynthesis of Ag-NP's. Among the various nanoparticles reported silver nanoparticle finds a tremendous application in the field of high sensitivity biomolecular detection and diagnostics [13], antimicrobials and therapeutic agent [14–19], catalysis [20], microelectronics [21], bio labelling and antimicrobials [22–25]. Silver nanoparticles have also become an essential component in clothing, food containers, wound dressings, ointments and implant coatings [26, 27], and some already approved from FDA [28]. Phytoconstitutents extracted from various plants are found to possess antitumor activity. Chemotherapy [29] is one of the traditional methods used for treatment of various forms of cancer; the drawback of chemotherapy is its inability to differentiate between normal and cancer cells. Any chemo preventive agent used should be capable of inhibiting cancer cell growth without affecting the normal cells. The potent antiangiogenic and anti-permeability effects of silver nanoparticles report that along with their ability to hold tumour progression in cancer cells [30] have prompted the study of the antitumor effect of the silver nanoparticles against DLA cell lines. DFT studies are carried out to explain the reducing ability of FHLE as a reducing agent to reduce Ag^{+} to Ag^{0}. The present study provides green biological route of synthesising silver nanoparticles using FHLE and for the first time the antitumor activity of FH mediated Ag-NP's are tested against DLA cell lines and DFT studies is carried out to reveal the reducing behaviour of FHLE to behave as a reducing agent in biosynthesis of Ag-NP's.

2 Materials and Methods

2.1 Preparation of FHLE

The fresh leaves of FH were obtained from Karpagam University Campus, Coimbatore. The fresh leaves were cleaned with deionized water to remove mud and other impurities and then it is cut into small pieces. The FHLE was prepared by placing 5 g of FH fine cut pieces and 500 ml double distilled water in a 1000 ml beaker and boiled for 5 min. The solution was cooled at room temperature. Following this extract was filtered through Whatman No. 1 filter paper and the resultant solution was refrigerated.

2.2 Biosynthesis of Silver Nanoparticles

The silver nitrate used in this experiment is obtained from Sigma-Aldrich. Figure 1 shows the schematic preparation of the stigmasterol mediated Ag-NP's. The silver nanoparticles is synthesised by adding 20 ml of FHLE to 80 ml of 10^{-3} M silver nitrate solution in a 250 ml capacity beaker and the reaction is left to take place at the ambient conditions. The light yellow coloured solution gradually turns to dark brown after 2 h which indicates the complete formation of silver nanoparticles. The progress of the reaction was monitored by using UV–visible (UV–Vis) spectral analysis. Once the solution reaches the dark brown colour it is then centrifuged at 5000 rpm in order to collect silver nanoparticles. The nanoparticle is washed with deionized water and stored in screw capped bottle for further characterisation.

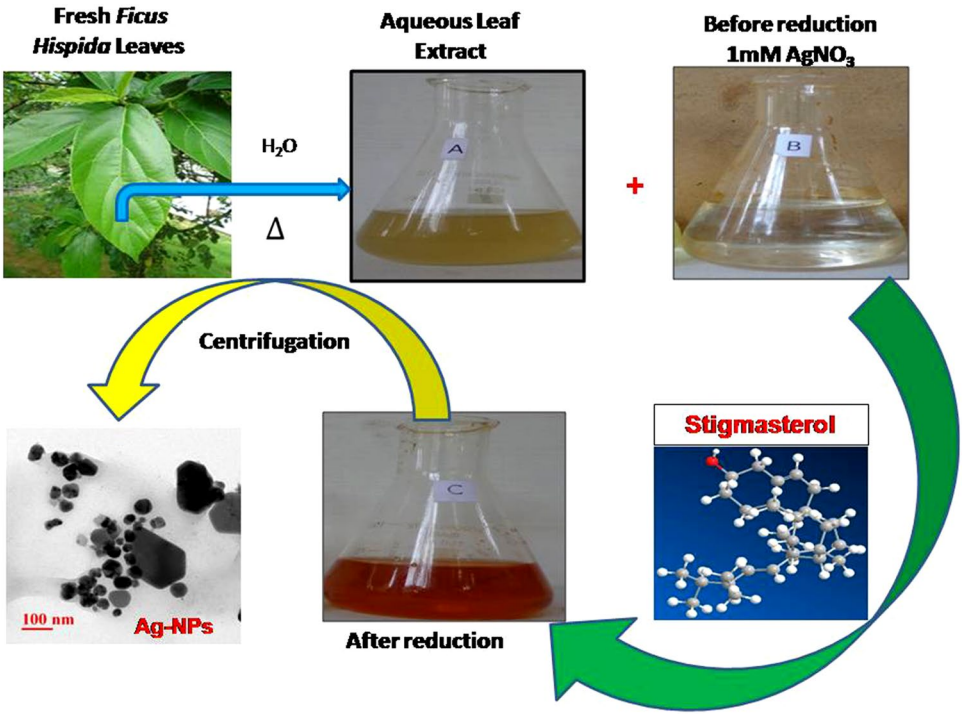

Fig. 1 The overall synthetic procedure of the Ag-NPs

Author's personal copy

2.3 Characterization of Silver Nano particles

2.3.1 Formation of Ag-NPs Monitored by UV–Vis Analysis

The colour change of the reaction mixture and formation of Ag-NP's is monitored by UV–Vis spectrum. The reaction mixture at regular time intervals is analysed using UV-1601 Shimadzu spectrophotometer and the spectrum was recorded.

2.3.2 Identification of Reductant Functional Group Using FT-IR Techniques

FT-IR spectra were recorded with the frequency ranging from 400 to 4000 cm^{-1} for the FH as well as the *Ficus* mediated Ag-NP's in KBr matrix using SHIMADZU-FTIR-8400S spectrophotometer instrument (Tokyo, Japan).

2.3.3 Size and Elemental Analysis

The synthesized nanoparticles is analyzed by quanta 200 FEG SEM instrument which is attached with EDX Analyzer as detector and employed using JEOL JED-2300analysis station at 20 keV, the SEM image and EDX spectrum of synthesised Ag-NP's is recorded.

2.3.4 HR-TEM Analysis

The synthesized Ag-NP's is further characterised for the size and shape using the HR-TEM and selected area electron diffraction (SAED) by JEOL JEM 2100 instrument. Silver nanoparticle is placed as a drop on the carbon-coated copper grid and allowed to dry at ambient temperature for 12 h and then analysed. The size of Ag-NP's in HR-TEM image is measured by using the image J software.

2.3.5 Analysis of Metal and Metal Oxide Phase by XRD Techniques

The formation of mono-phase compound is checked by XRD techniques. *Ficus* mediated Ag-NP's are washed thoroughly in the triple distilled water centrifuged and dried at 30 °C. The purified Ag-NP's are analyzed with XRD analysis by XRD Gonimeter, (SHIMADO-Model XRD 6000). The scanning is done in the region of 2θ from 20° to 80 °C at 0.02°/min and the time constant was 2 s.

2.3.6 Antitumor Activity of Biosynthesised Ag-NP's

The antitumor assay of FH mediated Ag-NP's are done by adding various concentrations of Ag-NPs ranging from 10 to 200 µg/ml to the tubes containing viable DLA cell suspension of 1×10^6 cells in 0.1 ml isolated from tumour bearing mice and volume of the tubes is made upto 1 ml using phosphate buffered saline (PBS) along with the control tube containing only DLA cell suspension and the mixture is incubated for 3 h at 37 °C and then 0.1 ml of 1% trypan blue dye suspension is added to the reaction mixture and kept for 2–3 min and then it is loaded in haemocytometer. Dead cells take the blue color of trypan blue while live cells do not take the dye. The number of stained and unstained cells are counted separately.

$$\% \text{ of cytotoxicity} = \frac{\text{Number of dead cells}}{\text{Number of live cells} + \text{Number of dead cells}} \times 100$$

2.3.7 Quantum Chemical Studies

GC-MS analysis of FHLE is found to contain Stigma sterol as main phytoconstituent with the retention time of 32.94 and peak area 82.38% along with other components as reported by Muthukrishnan et al. [31]. Theoretical calculations are carried out by using the density functional theory (DFT) with Guassian 09 W program [32] for basis set of b3lyp/6-31g(d) for all the atoms in stigmasterol molecules (optimized molecular structure) as shown in the Fig. 2. The molecular structure and electronic properties of the stigmasterol have completely optimised using the DFT for all atoms of molecules. The quantum chemical parameters such as energy of the highest occupied molecular orbital (E_{HOMO}), energy of the lowest unoccupied molecular orbital (E_{LUMO}), dipole moment (D) and the energy gap (ΔE) is determined.

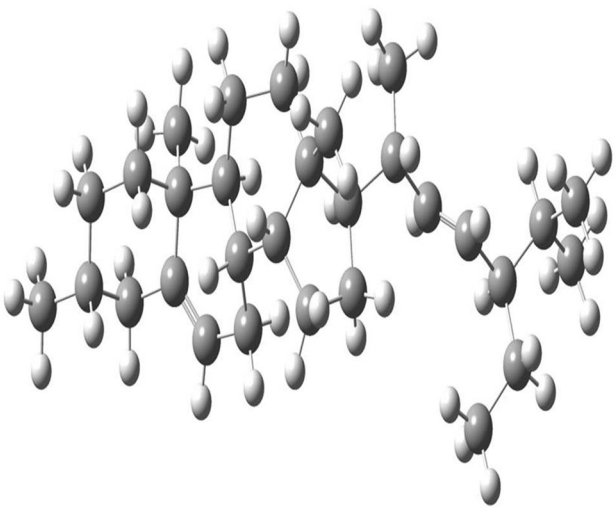

Fig. 2 Optimized molecular structure of stigmasterol

Author's personal copy

3 Results and Discussion

3.1 UV–Vis Spectra

The formation and stability of Ag-NP's is confirmed by UV–Vis spectral technique. When varying concentration of $AgNO_3$ is added to the FH leaf extract. The colour change of the reaction mixture indicates the formation of Ag-NPs. The UV–Vis spectra is used to monitor the progress of reaction with respect to time and also with different concentration of $AgNO_3$ as shown in the Fig. 3a (time variation) and Fig. 3b (concentration variation). The Fig. 3a depicts the UV–Vis spectra of Ag-NPs formation at 1 mM $AgNO_3$ under various time intervals such as 0–150 min. The silver SPR band occurs at 448 nm and intensity of the absorption increases with time. The observed colour change of the reaction mixture is from pale yellow to dark brown colour. These colour changes occur due to the surface resonance vibrations of the biosynthesised Ag-NPs. The surface plasmon resonance (SPR) bands are responsible for the dark brown colour reaction mixture which takes place as a result of interaction of electromagnetic field with free conduction electrons. The various concentration of leaf extract from 2.5 to 12.5% is added to 1 mM $AgNO_3$ as shown in the Fig. 3b. It is observed that SPR band at 448 nm steadily increases with the intensity irrespective to the different concentrations of the added $AgNO_3$ and does not show any shift in wavelength. Prakash et al. [25] report the reduction of argen ion and formation of Ag-NPs are found to take place within 3 h. In the present work, UV–Vis spectra are recorded to monitor the reaction in every 15 min time interval and the absorption peak steadily increases with time. However, the intensity of colour does not intensify even after 24 h as established by UV–Vis spectra. The obtained UV–Vis spectrum reveals that the reaction which is completed after 150 min as the spectrum does not show any increase in intensity of absorption after 150 min. UV–Vis spectrum recorded after 60 days does not show any shift in absorption wavelength and intensity which is very supportive and convenient for the synthesis of Ag-NPs.

3.2 Role of IR Spectrum in Predicting the Role of Functional Groups in Bioreduction of Silver Nitrate

FT-IR measurements are done to identify the various functional groups responsible for synthesis and stabilization of nanoparticle. FT-IR spectra of the FHLE and biosynthesized silver nanoparticles are shown in the Fig. 4a, b. FT-IR spectra of the FH spectra reveals several absorption bands at 3383, 2926, 2350, 1625, 1402, 1060 cm^{-1} along with other small bands. These bands corresponds to –OH and/or –NH, C–H bending modes in the hydrocarbon chains, C=O group, C=C stretching, C–OH stretching vibrations, C–O stretching and C–H bend of alkynes. FT-IR spectra of Ag-NPs indicates the presence of broad peak at 3377 cm^{-1} which is due to stretching vibrations of hydroxyl groups (–OH) groups. A weak absorption at 2939 cm^{-1} could be assigned to aliphatic C–H stretching vibrations. The peak at 2357 cm^{-1} attributes to C–H asymmetric stretching. The strong absorption band at 1595 cm^{1} is due to C=C stretching vibrations of aromatic ring. The peak 1411 cm^{-1} may be due to –OH bending vibrations of polyols. The peak appearing at 1085 cm^{-1} corresponds to C–O stretching vibrations of phenolic groups. Moreover the peak at 927 cm^{-1} is because of R–C–H deformation of $=CH_2$. The band at 837 and at

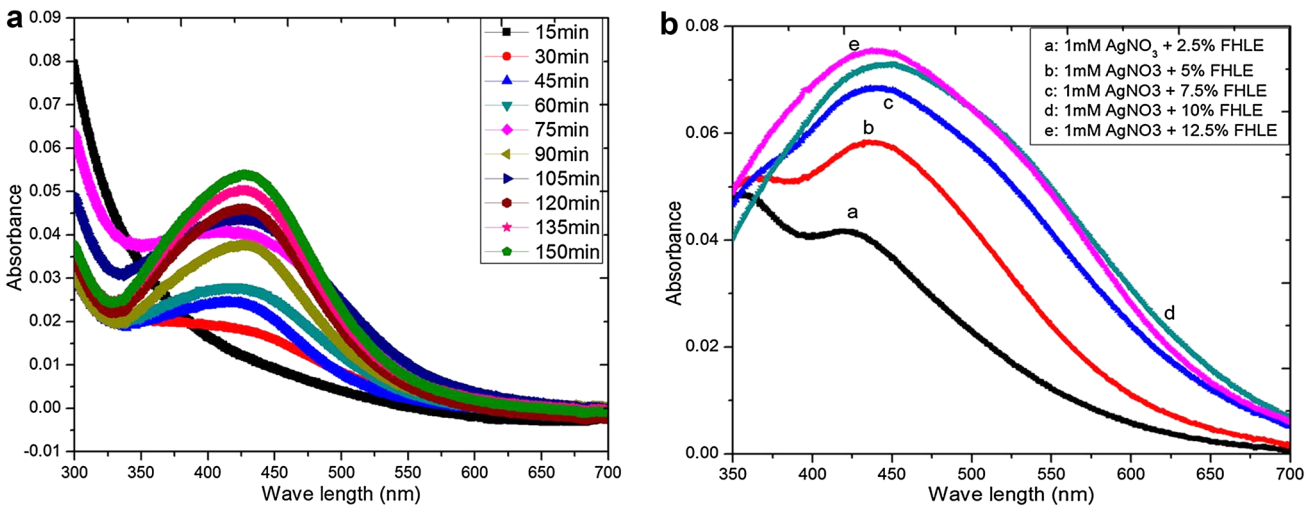

Fig. 3 Uv–Vis spectra depicting the formation and stability of silver nanoparticles at different time intervals (**a**) and at various concentrations of FHLE (**b**)

Author's personal copy

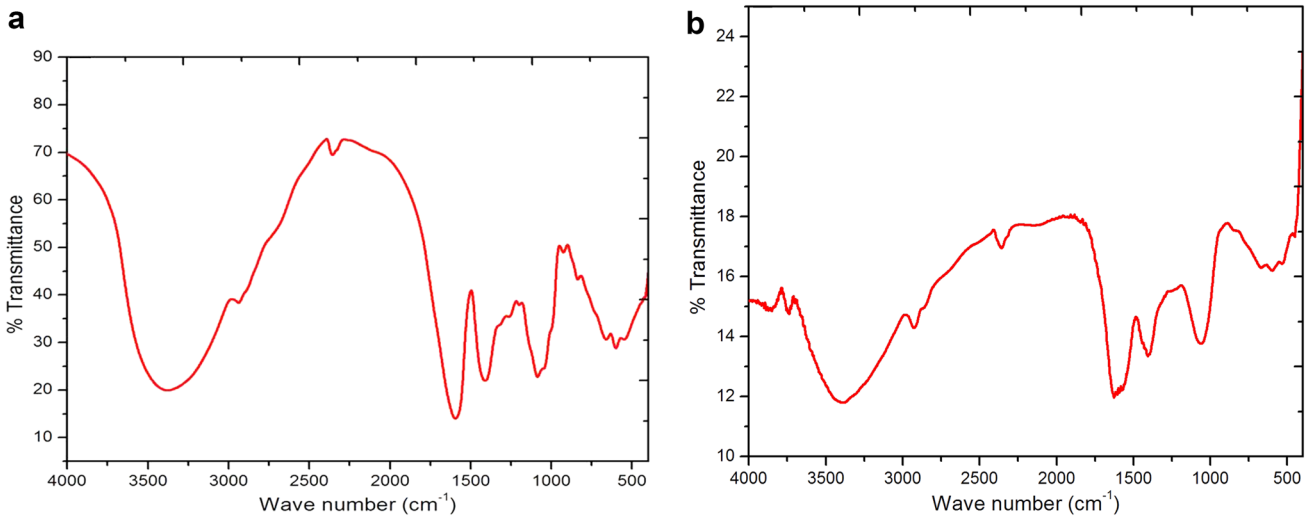

Fig. 4 FT-IR Spectra of **a** FHLE, **b** synthesized Ag-NPs with assisted FHLE

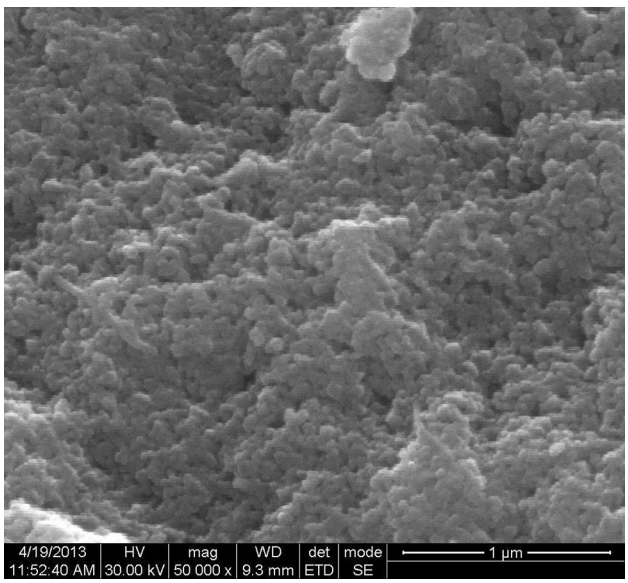

Fig. 5 HR-SEM photographs of the FH mediated Ag-NPs

600 cm^{-1} could be assigned for –C–H bending of alkynes.. In this study, the supplier of electrons is FH and the accepter was the Ag^{+} ions in aqueous silver nitrate solutions. Thus, it is proved that, only on the basics of the interactions between the donor and the acceptor, the reduction of Ag^{+} ions into Ag^{0} takes place.

3.3 HR-SEM and EDX Studies

The particle size and purity of Ag-NP's can be illustrated by SEM and EDX analysis. The Fig. 5 represents the SEM image of Ag-NPs synthesized by the FHLE and confirms the particle size in the range of 20–25 nm. In the present EDX analysis shown in The Fig. 6 shows high percentage of silver indicating the purity of synthesized sample. The EDX spectrum also reveals that the major peak is due to the metallic silver confirming the formation of silver nanoparticles.

3.4 HR-TEM Analysis and SAED Pattern

The size, shape and distribution of silver nanoparticles play a vital role in modulating their optical properties. The size and morphology of the synthesised silver nanoparticles by FHLE are characterized by TEM images as shown in the Fig. 7. The TEM images confirms the particle size of Ag-NPs ranging from 50 to 100 nm, homogenously distributed and have spherical shape. A clear lattice fringe of typical SAED pattern (Fig. 7d) reveals that the circular rings obtained corresponds to planes of 111, 200, 220, respectively shows Ag-NPs are highly crystalline that supports the results of XRD analysis.

3.5 XRD Studies

The crystalline nature of biosynthesised Ag-NP's are revealed by XRD analysis as shown in the Fig. 8. The observed diffraction peaks at 2θ value of 27.50°, 32.10°, 37.8°, 46.4° and 77.1°, these values corresponds with planes of 111, 200, and 220 respectively. The results show a good agreement with standard data (JCPDS: 01-087-0717) and the studies provides strong evidence that synthesised Ag-NPs have face centred cubic (FCC) structure of the metallic silver. The diffraction peaks at 27.50°, 32.10° is may be due to crystalline and amorphous organic phase.

Author's personal copy

Fig. 6 EDX spectra of Ag-NPs

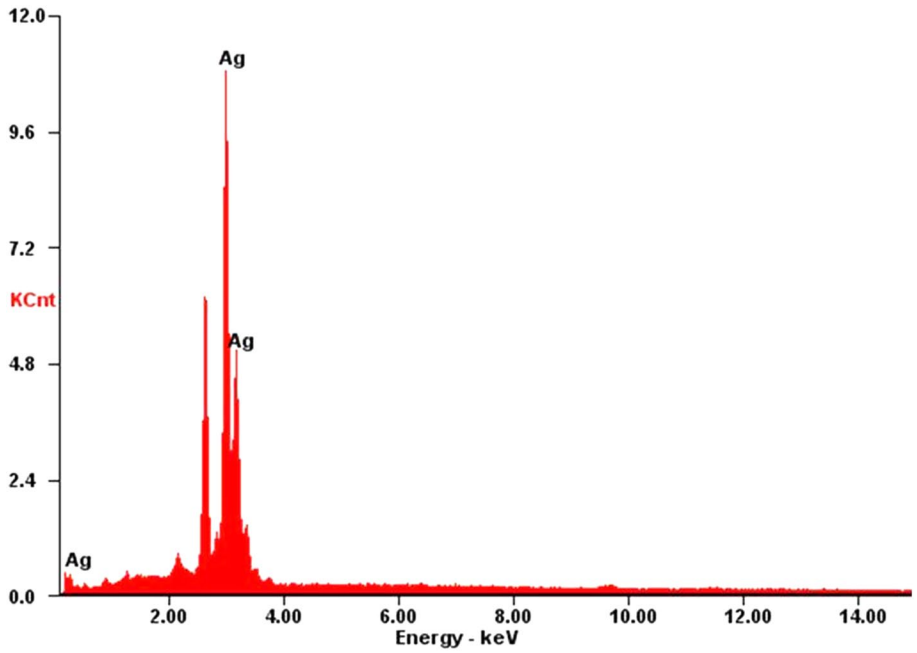

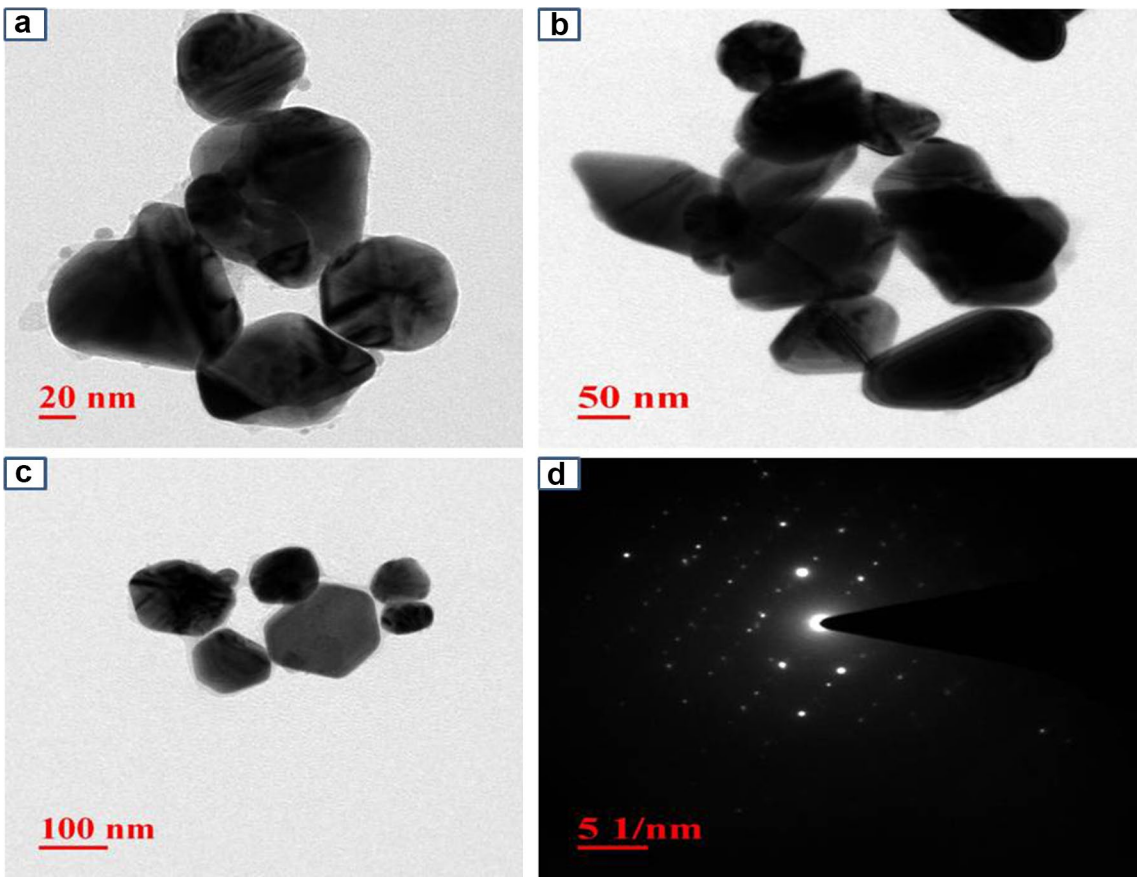

Fig. 7 Represents of TEM images **a** 20 nm, **b** 50 nm, **c** 100 nm **d** SAED patterns of as-synthesized Stigmasterol mediated Ag-NPs

Author's personal copy

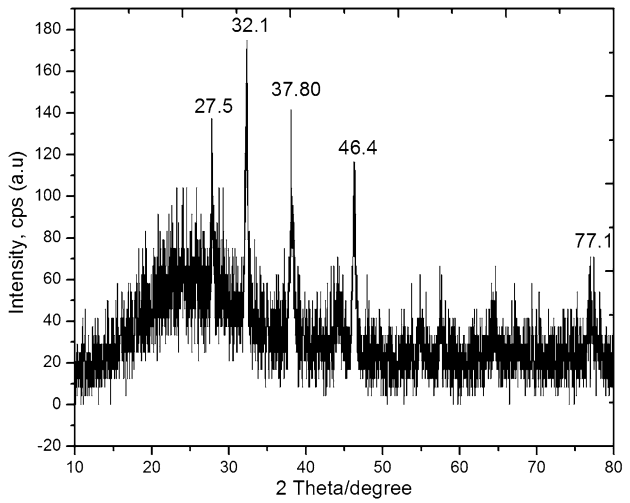

Fig. 8 XRD patterns of nano silver

Table 1 Effect of stigmasterol mediated Ag-NPs on the DLA cell lines

S. No.	Ag-NPs concentration (µg/ml)	% Cell death (DLA)	
		Ag-NPs	Standard drug Curcumin
1	10	18	41
2	20	20	54.47
3	50	48	69.71
4	100	70	81.69
5	200	100	100

3.6 Short Term In Vitro Cytotoxicity Assay

The anti-cancer activity of the various plant extract mediated synthesis of silver nanoparticles have been reported in previous studies [33–36]. But the invitrocytotoxicity of FH mediated Ag-NPs have not been reported. Trypan blue dye exclusion method is used to assess the cytotoxicity assay of biosynthesised Ag-NPs. Viable cells which remained unstained by trypan blue are counted by haemocytometer. Cytotoxicity of Ag-NPs synthesized using FH is shown in the Table 1. The percentage cytotoxicity of the DLA cells increased by increasing the concentration of Ag-NPs from 10 to 200 µg/ml. This study reveals that the complete inhibition of DLA cells takes place at 200 µg/ml as shown in the Fig. 9a, b. Curcumin was used as a reference drug and the percentage cytotoxicity of *Ficus* mediated silver nanoparticles was compared against the standard drug as shown in Table 1. This study provides evidence that FH mediated synthesised Ag-NPs show same 100% activity at 200 µg/ml as compared with the standard drug Curcumin [37].

3.7 Quantum Chemical Study of Stigmasterol

The reduction behaviour of stigmasterol present in FHLE can be ascertained by density functional studies (DFT) studies. The quantum indices like E_{HOMO}, E_{LUMO}, ΔE, dipole moment (µ), Ionisation potential and electron affinity are presented in the Table 2. Frontier orbital theory helps to understand the adsorption centres present in stigmasterol present in FHLE and their interaction with the surface of $AgNO_3$. The outermost orbital in the molecule is HOMO which is rich in electron and has the tendency to donate electrons and LUMO is the innermost lower energy orbital which is capable of receiving electrons. The presence of HOMO and LUMO orbitals in the molecule reveal their interaction with other reactants. The value of E_{HOMO} and E_{LUMO} play an important role in explaining the reaction behaviour of molecule. Higher the value of E_{HOMO} will be greater than the electron donating ability and lower E_{LUMO} values indicates the electron is the receiving ability [38]. The value of ΔE (energy gap) gives an idea of minimum amount of energy required to remove electron from the last occupied orbital (HOMO) and also the stability of the complex formed [39]. The decrease in the value of ΔE indicates the less amount of energy is only required to remove the electron from the outer most orbital (HOMO) of the molecule and also increases the stability of the complex formed. In the present study E_{HOMO} value of − 6.06 eV indicates that stigmasterol gets adsorbed on the surface of $AgNO_3$ and cause the reduction of Ag^+ to Ag^0. The HOMO orbitals (Fig. 10) are residing on –OH group side of the molecule and gives an clear explanation that lone pair of electrons on the oxygen atom enhances the electron donating ability. E_{LUMO} value of 0.77 eV and LUMO orbitals (Fig. 11) of the stigmasterol is deficient centre and the values of E_{HOMO} and E_{LUMO} indicate the binding ability of the FHLE to the surface of the metal halide and greater reducing ability to reduce the metal ions. The lower value of ΔE (− 6.83 eV) indicates that the only minimum amount of energy is alone required to remove the electron from oxygen atom which results in increased reducing ability to reduce Ag^+ to Ag^0. The values of dipole moment, ionisation potential and electron affinity values are presented in the Table 2 provides evidence that stigmasterol is bound strongly to the metal halide and thereby increasing reducing ability of the metal halide to metal nanoparticle.

4 Conclusion

For the first time rapid biological synthesis of Ag-NPs using with FHLE is reported. FT-IR, UV–Vis, SEM, TEM and XRD techniques confirmed the formation of silver nanoparticles with average size in the range of 50–100 nm. This present work provides that FH can be considered as one

Author's personal copy

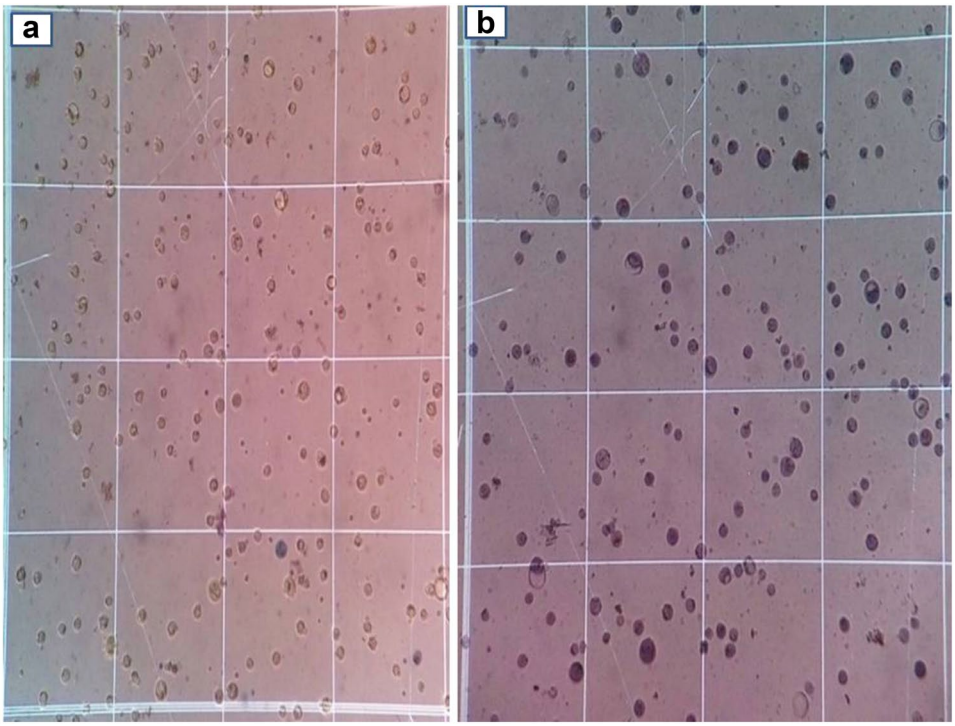

Fig. 9 In vitro toxicity assay of Ag-NPs using tryphan blue dye exclusion method against DLA cells (100% live cells: **a** white transparent cells and 100% dead cells: **b** dark opaque cells)

Table 2 Quantum chemical parameters of stigmasterol

Parameters	Calculated values
E_{HOMO}	− 6.06 eV
E_{LUMO}	0.77 eV
ΔE (E_{HOMO}–E_{LUMO})	− 6.83 eV
Dipole moment (D)	0.4124
Ionization potential	7.373 eV
Electron affinity	− 1.88 eV

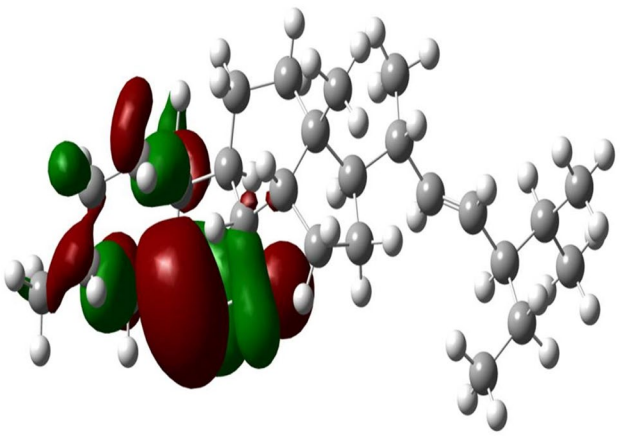

Fig. 10 Illustration of HOMO of the stigmasterol

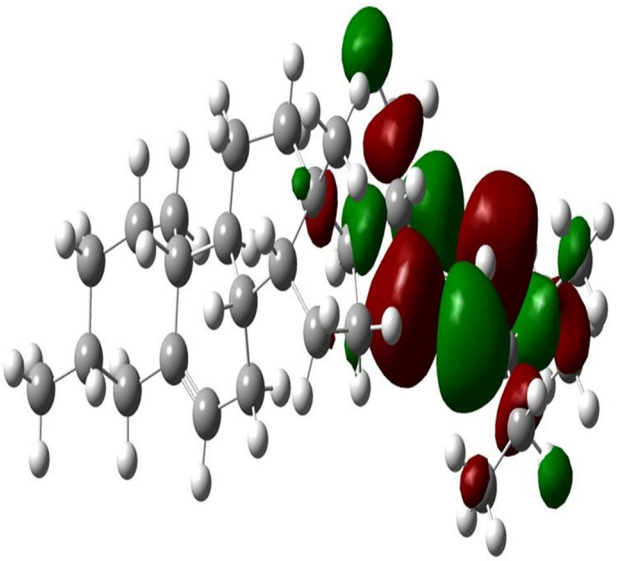

Fig. 11 Images of LUMO of the stigmasterol

of potential plants in the future for the production of silver nanoparticles. The DFT studies reveal that the stigmasterol presented in the FHLE play a vital role in reducing $AgNO_3$ and also behave as a better stabilising agent. The present study explores the antitumor activity of biosynthesised Ag-NPs in DLA cell lines and can be used as alternate therapeutic agent for the treatment of cancer. The green chemistry approach in synthesising Ag-NPs can be employed for the

Author's personal copy

large scale production of silver nanoparticles and finds large scope in the field of environmental protection.

References

1. A. Prabhu, K. Shankar, P. Muthukrishnan, A. Kathiresan, P. Prakash, Indo Am. J. Pharm. Res. **3**, 37 (2016)
2. B. Ankamwar, E-J.Chem. **7**, 1334 (2010)
3. Q.Y. Deng, B. Yang, J.F. Wang, C.G. Whiteley, X.N. Wang, Biotechnol. Lett. **10**, 1505 (2009)
4. R. Sathyavathi, M. Balamurali Krishna, S. Venugopal Rao, R. Saritha, D. Narayana Rao, Adv. Sci. Lett. **3**, 138 (2010)
5. S.J. Henley, J.D. Carey, S.R.P. Silva, Appl. Phys. Lett. **89**, 183120 (2006)
6. D.D. Evanoff Jr, G. Chumanov, Chem. Phys. Chem. **6**, 1221 (2005)
7. T.M. Tolaymat, A.M. El Badawy, A. Genaidy, K.G. Scheckel, T.P. Luxton, M. Suidan, Sci. Total Environ. **408**, 999 (2010)
8. M.G. Guzmán, J. Dille, S. Godet, World Acad. Sci. Eng. Technol. **43**, 357 (2008)
9. S. Navaladian, B. Viswanathan, R.P. Viswanath, T.K. Varadarajan, Nanoscale Res. Lett. **2**, 44 (2007)
10. K.J. Sreeram, M. Nidhin, B.U. Nair, Bull. Mater. Sci. **31**, 937 (2008)
11. R. Zamiri, A. Zakaria, H. Abbastabar, M. Darroudi, M. Shahril Husin, M.A. Mahdi, Int. J. Nanomed. **6**, 565 (2011)
12. M. Sastry, A. Ahmad, M. Islam Khan, R. Kumar, Curr. Sci. **85**, 162 (2003)
13. S. Schultz, D.R. Smith, J.J. Mock, D.A. Schultz, Proc. Natl. Acad. Sci. USA **97**, 996 (2000)
14. M. Rai, A. Yadav, A. Gade, Biotechnol. Adv. **27**, 76 (2009)
15. J.L. Elechiguerra, J.L. Burt, J.R. Morones, A. Camacho-Bragado, X. Gao, H. Lara, M.J. Yacaman, J. Nanobiotechnol. (2005). doi:10.1186/1477-3155-3-6
16. R. Emmanuel, P. Selvakumar, S.M. Chen, K. Chelladurai, S. Padmavathy, M. Saravanan, P. Prakash, M. Ajmal Ali, F.M. Al-Hemaid, Mater. Sci. Eng. C **56**, 374 (2015)
17. S. Arokiyaraj, V. Dinesh Kumar, V. Elakya, T. Kamala, S.K. Park, M. Ragam, M. Saravanan, M. Bououdina, M.V. Arasu, K. Kovendan, S. Vincent, Environ. Sci. Pollut. Res. Int. **22**, 9759 (2015)
18. S. Arokiyaraj, S. Vincent, M. Saravanan, Y. Lee, Y.K. Oh, K.H. Kim, Artif. Cell Nanomed. Biotechnol. **45**, 372 (2017)
19. K. Muthupandi, M. Saravanan, P. Prakash, H. Kumar, M. Ovais, H. Barabadi, Z. Khan, J. Interdiscip. Nanomed. **2**, 131 (2017)
20. R.M. Crooks, B.I. Lemon, L. Sun, L.K. Yeung, M. Zhao, Top. Curr. Chem. **212**, 82 (2001)
21. P. Raveendran, J. Fu, S.L. Wallen, Green Chem. **8**, 34 (2006)
22. P. Magudapathy, P. Gangopadhyay, B.K. Panigrahi, K.G.M. Nair, S. Dhara, Phys. B **299**, 142 (2001)
23. R. Joerger, T. Klaus, C.G. Granqvist, Adv. Mater. **12**, 407 (2000)
24. S. Arora, J. Jain, J.M. Rajwade, K.M. Paknikar, Toxicol. Lett. **179**, 93 (2008)
25. P. Prakash, P. Gnanaprakasam, R. Emmanuel, S. Arokiyaraj, M. Saravanan, Colloids Surf. B **108**, 255 (2013)
26. K. Muthupandi, P. Prakash, M. Saravanan, M. Mahalakshmi, Microb. Pathog. **107**, 327 (2017)
27. A. Kumari, P. Kumar, P.M. Ajayan, G. John, Nat. Mater. **7**, 236 (2008)
28. K. Dunn, V. Edwards-Jones, Burns 30, S1 (2004)
29. I.F. Tannock, R.P. Hilp, *The basic Science of Oncology*, 4th edn. (McGraw Hill, New York, 2007)
30. J.K. Srivasthava, S. Gupta, Biochem. Biophys. Res. Commun. **346**, 447 (2006)
31. P. Muthukrishnan, P. Prakash, B. Jeyaprabha, K. Shankar, Arab. J. Chem. (2015). doi.10.1016/j.arabjc.2015.09.005
32. M.J. Frisch, G.W. Trucks, H.B. Schlegel, G.E. Scuseria, M.A. Robb, J.R. Cheeseman, G. Scalmani, V. Barone, B. Mennucci, G.A. Petersson, H. Nakatsuji, M. Caricato, X. Li, H.P. Hratchian, A.F. Izmaylov, J. Bloino, G. Zheng, J.L. Sonnenberg, M. Hada, M. Ehara, K. Toyota, R. Fukuda, J. Hasegawa, M. Ishida, T. Nakajima, Y. Honda, O. Kitao, H. Nakai, T. Vreven, J.A. Montgomery Jr, J.E. Peralta, F. Ogliaro, M.J. Bearpark, J. Heyd, E.N. Brothers, K.N. Kudin, V.N. Staroverov, R. Kobayashi, J. Normand, K. Raghavachari, A.P. Rendell, J.C. Burant, S.S. Iyengar, J. Tomasi, M. Cossi, N. Rega, N.J. Millam, M. Klene, J.E. Knox, J.B. Cross, V. Bakken, C. Adamo, J. Jaramillo, R. Gomperts, R.E. Stratmann, O. Yazyev, A.J. Austin, R. Cammi, C. Pomelli, J.W. Ochterski, R.L. Martin, K. Morokuma, V.G. Zakrzewski, G.A. Voth, P. Salvador, J.J. Dannenberg, S. Dapprich, A.D. Daniels, Ö. Farkas, J.B. Foresman, J.V. Ortiz, J. Cioslowski, D.J. Fox, *Gaussian Revision C.01* (Gaussian Inc., Wallingford, 2009)
33. S. Bhuvaneshwari, S. Murugesan, Bangladesh J. Pharmacal. **7**,173 (2012)
34. S. Gurunathan, K.J. Lee, K. Kalishwaralal, S. Sheikpranbabu, R. Vaidyanathan, S.H. Eom, Biomaterials **30**, 6341 (2009)
35. M. Ovais, A.T. Khalil, A. Raza, M. Adeep Khan, I. Ahmad, N.U. Islam, M. Saravanan, M. Furqan Ubaid, M. Ali, Z.K. Shinwari, Nanomedicine **11**, 3157 (2016)
36. S. Gurunathan, J.H. Park, J.W. Han, J.H. Kim, Int. J. Nanomed. **10**, 4203 (2015)
37. M. Vishnu Kiran, S. Murugesan, World J. Pharm. Sci. **2**, 96 (2014)
38. M. Raafat, K. Mohamed, F. Awad, M. Atlam, Appl. Surf. Sci. **255**, 2433 (2008)
39. G. Guo, L. Chenghao, Electrochim. Acta **52**, 4554 (2007)